AIAA '89

AIAA 89-0159
Interaction of Droplet Clouds with Swirling Flows

M. Yang and M. Sichel, Univ. of Michigan, Ann Arbor, MI

27th Aerospace Sciences Meeting

January 9–12, 1989/Reno, Nevada

Interaction of Droplet Clouds with Swirling Flows

M. H. Yang and M. Sichel

Department of Aerospace Engineering
The University of Michigan
Ann Arbor, Michigan 48109

ABSTRACT

The momentum interaction of a cylindrical droplet cloud entrained in a forced or potential vortex is investigated in the present study. A cloud expansion time scale $\bar{\tau}_0/\varepsilon_v$ is first identified, then a dimensionless parameter σ, equal to the ratio of the cloud expansion time to the diffusion time is found to characterize the behavior of a droplet-laden swirling cloud. For the case of $\sigma \ll 1$ the forced vortex strength, even decreases due to the droplet drag on the gas flow, remains uniform within the initial cloud region. On the other hand, the droplets in the potential vortex essentially behave in a non-interactive mode so that the vortex decay is mainly caused by the viscous stress in itself rather than the existence of droplets. Besides, the parameter σ has implications for the cloud vaporization behavior considering $Pr = O(1)$. The results for $\sigma \ll 1$ suggests that a "strong" swirling flow may substantially influence the structure of the group vaporization or combustion. Finally the approximate analytical solutions developed for $\sigma \ll 1$ are found to be in excellent agreement with numerical solutions.

NOMENCLATURE

Dimensional Variables

$\bar{D}$	Droplet diameter
$\bar{K}$	Evaporation constant
$\bar{k}$	Vortex strength
$\bar{l}$	Inter-droplet distance
$\bar{n}$	Number density
$\bar{R}$	Cloud radius
$\bar{r}$	Radius
$\bar{t}$	Time
$\bar{U}$	Droplet velocity
$\bar{V}$	Gas velocity
$\bar{\mu}$	Gas viscosity coefficient
$\bar{\nu}$	Gas kinematic viscosity
$\bar{\rho}$	Density
$\bar{\tau}$	Velocity relaxation time
$\bar{\delta}$	thickness of the vaporization layer

Dimensionless Variables

Cd	Drag coefficient
D	$= \bar{D}_d/\bar{D}_{d0}$
K	$= \bar{K}\,\bar{\tau}_0/\bar{D}_{d0}^2$
K'	$= K(1 + 0.276\,Re^{1/2}\,Pr^{1/3})$
k_f, k_{fr}	defined in Eq. (13)
k_p, k_{pr}	defined in Eq. (23)
n	$= \bar{n}/\bar{n}_0$
Pr	Prandtl number
Re	Reynolds number
r	$= \bar{r}/\bar{R}_0$
t	$= \bar{t}/(\bar{\tau}_0/\varepsilon_v)$
U_r	$= \bar{U}_r/(\varepsilon_v\bar{R}_0/\bar{\tau}_0)$
U_θ	$= \bar{U}_\theta/(\bar{k}_{f0}\bar{R}_0)$ or $\bar{U}_\theta/(\bar{k}_{p0}/\bar{R}_0)$
V_r	$= \bar{V}_r/(\varepsilon_v\bar{R}_0/\bar{\tau}_0)$
V_θ	$= \bar{V}_\theta/\bar{k}_{f0}\bar{R}_0)$ or $\bar{V}_\theta/(\bar{k}_{p0}/\bar{R}_0)$
β	$= \frac{1}{6}\pi\bar{n}\bar{\rho}_d\bar{D}_d^3/\bar{\rho}_g$
β'	$= (1 + \frac{3}{2}K')\beta$
ε_c	$= (2\pi\bar{n}_0\bar{D}_{d0}\bar{R}_0^2)^{-1}$
ε_v	$= (\bar{k}_{f0}\bar{\tau}_0)^2$ or $(\bar{k}_{p0}\bar{\tau}_0/\bar{R}_0^2)^2$
σ	$= (\bar{\tau}_0/\varepsilon_v)/(\bar{R}_0^2/\bar{\nu})$
τ	$= \bar{\tau}/\bar{\tau}_0$
ρ_g	$= \bar{\rho}_g/\bar{\rho}_{g0}$
θ	Angular displacement
υ	Volume of the discrete cell
Δ	$=(k_{f0}-k_f)/k_f$ or a difference operator

Subscripts

0	Initial condition
d	Droplet
f	Forced vortex
g	Gas
p	Potential vortex
r	Radial direction
θ	Tangential direction

INTRODUCTION

In most liquid fuel combustion systems a spray is injected through an atomizer into a chamber, where it mixes with the ambient gas and burns. Experiments[1,2] have revealed that the combustion of droplets in a spray differs fundamentally from the combustion of an isolated droplet. The collective behavior of droplets in a spray usually results in a relatively cool and fuel-rich region. The droplets in this region first vaporize and

the vapor then burns as a gas-phase diffusion flame outside the droplet cloud; in other words, the droplets in the spray vaporize or burn as a group rather than as individual droplets.

The concept of the group behavior of droplet clouds in a stationary atmosphere has by now been well established.[3-7] The effect of convective flow on droplet cloud behavior has been studied by Bellan and Harstad.[8,9] However, droplet clouds in swirling flows have rarely been investigated even though swirl combustors,[10] swirl atomizers,[11] swirl diffusion flames[12] and swirl mixing[13] have recently gained considerable attention. Mao et al.[11] have found in recent experiments that swirl spray flames have a different structure from non-swirl spray flames or regular turbulent diffusion flames. In a previous study[14] the behavior of a dilute cloud in both forced and potential vortices has been studied, and it was concluded that the droplet density redistribution in the cloud may significantly influence the structure of the group vaporization or combustion.

This paper is focused on droplet clouds in axisymmetric swirling flows, in particular on the interaction between the droplets and the gas flow. The momentum interaction between the two phases is in general attributed to three components: (1) the droplet drag, (2) the droplet vaporization, and (3) a small pressure gradient.[9] Previous analytical studies[15-17] of the droplet motion in swirling flows have generally neglected all interaction effects since the inclusion of any of these effects will certainly complicate the problem. Fortunately it has been found that a nondilute spray only requires a few milli-seconds to attain a near-saturated condition, and only a small fraction of a second to reach complete saturation within the cloud.[18] It is then reasonable to assume that the cloud is initially in the near-saturated condition so that the vaporization effect on the interior gas motion is small. In the present study the momentum exchange due to the droplet drag and slow vaporization will be evaluated while the pressure is assumed constant.

The governing equations for the swirling droplet clouds are first formulated below and are used to identify characteristic time scales associated with the swirling clouds. It is shown that the behavior of the swirling cloud is characterized by a parameter equal to the ratio of a characteristic cloud expansion time to a characteristic diffusion time. The governing equations are then used to study the effect of gas-droplet interaction on forced and potential vortex droplet clouds.

GOVERNING EQUATIONS AND CLOUD CHARACTERISTICS

The behavior of a dilute cylindrical droplet cloud in swirling flows has been analyzed elsewhere[14] by assuming time-invariant forced and potential vortices. The present analysis is mainly concerned with the momentum interaction between a cylindrical droplet cloud and the swirling flow of an infinitely large region (see Fig. 1), as well as the characterization of droplet-laden swirling flows by suitable dimensionless parameters. As discussed above it can be assumed that the swirl cloud is initially in a near-saturated state so that the radial velocity (Stefan flow) of the vapor is small. It is not clear how long it will take the swirl cloud to reach complete saturation or if it ever does so. In this study the droplets within the cloud are assumed to evaporate slowly. The mass loading ratio (liquid mass/gas mixture mass) within the cloud is assumed to be in the range of 0.1 ~ 10. The initial swirling gas flow is that of an axisymmetric forced or potential vortex. The analysis of other more complex swirling flows such as a Rankine or Hill spherical vortex is not attempted here.

The major assumptions made in this analysis are: (1) the density ratio ($\bar{\rho}_d/\bar{\rho}_{g0}$) is of the order of 1000, (2) the droplet mass loading ratio is assumed not to exceed 10 so that the volumetric fraction of the droplets can be neglected, (3) the droplet vaporization rate within the spray is assumed small, (4) the droplet temperature is constant and uniform, (5) the droplets are mono-sized and initially uniformly distributed within the cloud, (6) the droplet interactions, breakup and collisions are neglected, (7) the radial velocity of vapor-gas mixture within the cloud is at least one order of magnitude less than that of the droplets.

1. Cloud Expansion Time Scale

In the previous non-interactive vortex cloud study[14,19] it was shown that an appropriate parameter governing the single droplet motion in an axisymmetric forced or potential vortex field is ε_v (= square of Stokes number) rather than the Stokes number itself. The Stokes number is defined as the ratio of the droplet velocity relaxation time to the characteristic flow time,[20] and is often used to indicate the ability of droplets to respond to changes in the gas flow. For forced and potential vortices the initial gas velocities are

$$\bar{V}_\theta = \bar{k}_{f0}\bar{r}, \quad \bar{k}_{p0}/\bar{r} \qquad (1a,b)$$

respectively and the corresponding values of the parameter ε_v are then

$$\varepsilon_v = (\bar{k}_{f0}\bar{\tau}_0)^2, \quad (\bar{k}_{p0}\bar{\tau}_0/\bar{R}_0^2)^2 \qquad (2a,b)$$

Here $\bar{\tau}_0 = \bar{\rho}_d\bar{D}_{d0}^2/(18\bar{\mu})$ is the initial velocity relaxation time for a single droplet. Typical values of $\bar{\tau}_0$ for 50 and 100 μm hydrocarbon fuel droplets in a boiling environment are about 5 and 20 msec respectively. Note that symbols are defined in the nomenclature.

For $\varepsilon_v \ll 1$, it follows from physical arguments that the droplet tangential velocity will rapidly relax to the gas tangential velocity, so that after a short time the droplet velocity becomes independent of the initial tangential velocity. For non-vaporizing droplets the radial velocity, to

zeroth order, in both forced and potential vortices can be shown to be respectively[14]

$$\bar{U}_r = (\varepsilon_v/\bar{\tau}_0)\bar{r}, \quad (\varepsilon_v/\bar{\tau}_0)(\bar{R}_0^4/\bar{r}^3) \qquad (3a,b)$$

Equations (3a,b) suggest that the initial cloud boundary at $\bar{r} = \bar{R}_0$ is expanding with velocity $(\varepsilon_v\bar{R}_0/\bar{\tau}_0)$, so that a characteristic cloud expansion time based on the cloud radius $\bar{R}_0$ can be defined as

$$\text{Cloud expansion time scale} = \bar{\tau}_0/\varepsilon_v. \qquad (4)$$

The role of the cloud expansion time scale in the case of vaporizing sprays will become evident after the nondimensionalization of governing equations.

2. Droplet Phase Equations

The droplet phase is treated in Lagrangian coordinates and as a continuum in the number density equation. Using the characteristic time $\bar{\tau}_0/\varepsilon_v$, length $\bar{R}_0$, radial velocity $\varepsilon_v\bar{R}_0/\bar{\tau}_0$ and tangential velocity $\bar{k}_{f0}\bar{R}_0$ or $\bar{k}_{p0}/\bar{R}_0$ for the forced and potential vortices, the droplet dynamic equations are non-dimensionalized to yield

$$\frac{dU_r}{dt} = \frac{1}{\varepsilon_v}\frac{U_\theta^2}{r} + \frac{1}{\varepsilon_v}\frac{V_r - U_r}{\tau} f(Re) \qquad (5a)$$

$$\frac{dU_\theta}{dt} = -\frac{U_r U_\theta}{r} + \frac{1}{\varepsilon_v}\frac{V_\theta - U_\theta}{\tau} f(Re) \qquad (5b)$$

$$dr/dt = U_r \qquad (6a)$$

$$r(d\theta/dt) = U_\theta/\varepsilon_v^{1/2} \qquad (6b)$$

and for the low Reynolds Number flow under consideration the viscous drag function is taken as $f(Re) = 1 + \frac{1}{6}Re^{2/3}$. It should be noted that the Basset force, pressure gradient force, apparent mass force and any other forces are neglected based on assumption (1)[21]; droplet-droplet interactions are neglected based on assumption (2), and the effect of droplet vaporization on the drag is also neglected based on assumption (3). Therefore, the droplet drag coefficient $Cd = (24/Re)f(Re)$ can be used with satisfactory accuracy.[22] Moreover, if $\varepsilon_v \ll 1$, which is the case of interest in this analysis, the relative velocity and hence the associated Reynolds No. will quickly relax to a value of $O(\varepsilon_v)$, so that the Stokes drag assumption $f(Re) = 1$ can be considered as a good approximation in Eq. (5). On the other hand, the variation of the droplet drag coefficient has to be considered more carefully if $\varepsilon_v \geq 1$.

Using the initial number density $\bar{n}_0$ and initial droplet diameter $\bar{D}_{d0}$ as reference values, the dimensionless droplet number density and vaporization equations are given by

$$\frac{dn}{dt} + \frac{n}{r}\frac{\partial(rU_r)}{\partial r} = 0 \qquad (7)$$

$$\frac{d\tau}{dt} = -\frac{K}{\varepsilon_v}(1+0.276\,Re^{1/2}\,Pr^{1/3}) = -\frac{K'}{\varepsilon_v} \qquad (8)$$

where K is the dimensionless vaporization constant. The dimensionless relaxation time τ, in fact, is the square of the dimensionless droplet diameter D_d^2 since $\tau = \bar{\tau}/\bar{\tau}_0 = (\bar{D}_d/\bar{D}_{d0})^2$. On the basis of assumption (4), it is reasonable to use the "D^2-law" of vaporization which is the basis of Eq. (8). It should be noted that $K \sim O(1)$ in single droplet combustion. However, $K \ll 1$ in the case of the slow vaporization considered here, and $K = 0$, so that $\tau = 1$ in the non-vaporizing case.

3. Gas Phase Equations

Since the gas radial velocity is small compared to the gas tangential velocity, the dimensionless θ-momentum equation for the gas becomes

$$\frac{\partial V_\theta}{\partial t} = -\frac{\beta}{\varepsilon_v}\frac{V_\theta - U_\theta}{\tau} f(Re) + \frac{3K'\beta}{2\varepsilon_v\tau}(U_\theta - V_\theta) + \frac{\sigma}{\rho_g}\frac{\partial}{\partial r}\left(\frac{1}{r}\frac{\partial}{\partial r}(rV_\theta)\right) \qquad (9)$$

β, the droplet loading ratio, the ratio of the spray mass per unit volume to the gas density, can be represented as

$$\beta = \frac{\beta_0 n \tau^{3/2}}{\rho_g} \qquad (10)$$

The first term on the right hand side of Eq. (9) represents the drag force of the droplets on the gas flow; the second term is the momentum source (sink) due to droplet vaporization. The third term is due to the gaseous viscous stress, and the coefficient σ in terms of dimensional quantities is given by

$$\sigma = \frac{\bar{\tau}_0/\varepsilon_v}{\bar{R}_0^2/\bar{\nu}_0} \qquad (11)$$

Therefore σ represents the ratio of the characteristic cloud expansion time to the characteristic viscous diffusion time (or say, vortex decay time). The relevance of this ratio to practical sprays becomes apparent when σ is expressed in alternate form after substituting for $\bar{\tau}_0$:

$$\sigma = \frac{1}{18\varepsilon_v}\frac{\bar{\rho}_d}{\bar{\rho}_{g0}}\frac{\bar{D}_{d0}^2}{\bar{R}_0^2} = \frac{2}{3}\beta_0\frac{\varepsilon_c}{\varepsilon_v} \qquad (12)$$

where $\varepsilon_c = (2\pi\bar{n}_0\bar{D}_{d0}\bar{R}_0^2)^{-1}$ has been used as a small parameter in the asymptotic analysis of spherical sheath combustion by Correa and Sichel.[5,6] The parameter ε_c is in fact the

inverse of the group combustion number proposed by Chiu and his coworkers,[3,4] and can be shown to be equal to $(\bar{\delta}/\bar{R}_0)^2$ where $\bar{\delta}$ is the thickness of the vaporization front at the edge of the cloud.[5,6] For the case of $\beta_0 = O(1)$ in the swirling cloud, the relative magnitudes of ε_c and ε_v will determine the significance of the gas viscous diffusion, and hence the significance of the gas thermal diffusion if $Pr = O(1)$ relative to the cloud expansion due to swirling flows.

The problem of the cloud behavior in swirling flows can now be categorized into various regimes according to the magnitude of σ. The analysis of the momentum interaction will be presented in the subsequent section.

(1) $\sigma << 1$

Gas diffusion velocity << Cloud expansion velocity

The viscous diffusion of the vortex flow in this regime is negligible. The gas velocity within the cloud is largely determined by the droplet drag and the vaporization source. When the droplets spiral out of the initial cloud, they may not survive for a significant time due to the heated ambience. The initial cloud region is therefore the main region within which the vortex velocity will govern the droplet motion and is the region which will be particularly discussed in this study. In the case of $\beta_0 = O(1)$, this regime implies $\varepsilon_c << \varepsilon_v << 1$, and this condition will be satisfied for relatively large values of k_{f0} or k_{p0}.

(2) $\sigma = O(1)$

Gas diffusion velocity ≈ Cloud expansion velocity

The decay of the vortex within the cloud is not only determined by the existence of droplets but also by the viscous stress within the ambient gas or the cloud itself. This regime is characterized by $\varepsilon_c \approx \varepsilon_v$ if $\beta_0 = O(1)$.

(3) $\sigma >> 1$

Gas diffusion velocity >> Cloud expansion velocity

The strength of the vortex is very limited. In the limiting case, the cloud becomes almost stationary so that the droplet motion becomes less important compared to the speed of the viscous or thermal diffusion. The vaporization behavior of the cloud is characterized by a regressive vaporization layer at the edge of the cloud. The speed of this thin layer is mainly determined by the parameter ε_c and the ambient conditions.[5,6] Therefore, it is better to use the diffusion time scale rather than the cloud expansion time scale to describe the vaporization behavior of the cloud. For $\beta_0 = O(1)$, then $\varepsilon_v << \varepsilon_c << 1$ in this regime.

The behavior of the cylindrical cloud in the regime of $\sigma >> 1$ is essentially similar to the spherical problem discussed by Correa and Sichel.[5,6] In the regime of $\sigma = O(1)$ numerical solutions are generally required. In the following the analytical results for the momentum interaction are developed for the regime of $\sigma << 1$.

For a typical example $\beta_0 = 1$, $\bar{D}_{do} = 100$ μm, $\bar{R}_0 = 10$ cm, then $\varepsilon_c = O(10^{-4})$. In the regime $\sigma << 1$, this implies $\varepsilon_v = O(10^{-2})$.

ANALYSIS AND RESULTS

1. Forced Vortex Cloud

The dimensionless gas velocity in a forced vortex is initially $V_\theta = r$ plus a small radial velocity. With the disturbance caused by droplets, it is not clear whether the gas tangential velocity remains linear with radius. However, the dimensionless gas velocities may still be expressed as

$$V_\theta = k_f r, \qquad V_r = k_{fr} \tau r \tag{13a,b}$$

Here k_f is not yet considered as an ordinary vortex strength, but as a general function of (r,t) defined by Eq. (13a). Also, k_{fr} is small compared with k_f and should be expressible as a function of k_f and droplet properties. It should also be noted that $k_{fr} = 0$ for the non-vaporizing cloud.

Without loss of generality, the radial and tangential velocities of droplets in Lagrangian coordinates can be written in the form

$$U_\theta = r h(t), \qquad U_r = r \tau g(t) \tag{14a,b}$$

where g and h are arbitrary functions of time and $r = r(t, r_0)$. In the Lagrangian formulation $(U_\theta, U_r, \theta, r, \tau)$ depend only on time if the initial droplet location r_0 is specified.

Substituting Eqs. (13,14) into Eq. (5) with the aid of Eqs. (6,8) yields the following equations for the functions $g(t)$ and $h(t)$.

$$\frac{dh}{dt} = \frac{1}{\varepsilon_v \tau}(k_f - h) - 2\tau g h \tag{15a}$$

$$\frac{dg}{dt} = \frac{1}{\varepsilon_v \tau}(h^2 - (1 - K')g + k_{fr}) - \tau g^2 \tag{15b}$$

The zeroth order solutions of Eq. (15) with $\varepsilon_v << 1$ are $h \approx k_f$, $g \approx (k_f^2 + k_{fr})/(1 - K')$. To first order in ε_v the solutions are then given by

$$h = k_f - \varepsilon_v h_1 \tag{16a}$$

$$g = (k_f^2 + k_{fr})/(1 - K') - \varepsilon_v g_1 \tag{16b}$$

where h_1 and g_1 are general functions of k_f and t and to be determined by solving the gas phase equation (9) and Eq. (15) together.

By neglecting the viscous term in the case of $\sigma << 1$ and substituting Eqs. (13a,14a,16a) into Eq. (9) and eliminating r from both sides of the equation, it follows that

$$\frac{\partial k_f}{\partial t} = -\left(1+\frac{3}{2}K'\right)\frac{\beta}{\tau}h_1 = -\left(1+\frac{3}{2}K'\right)\frac{\beta_0 n_f \tau^{1/2}}{\rho_g}h_1 \qquad (17)$$

Four variables (K', k_f, n_f, τ) are functions of (r,t). However, Eq. (17) suggests that if K', n_f, τ are uniform, then k_f will also be uniform (independent of r). Meanwhile Eq. (7) for the number density suggests that if K', k_f, τ are uniform, then after the substitution of $U_r \approx (k_f^2+k_{fr})\tau r/(1-K')$, n_f becomes independent of r_0 in Lagrangian coordinates and thus will also be uniform in Eulerian coordinates.

For the regime $\sigma << 1$, the temperature within the cloud is mainly determined by the vaporization of droplets, and since K' is mainly a function of temperature, the uniform n_f, τ will cause K' to be uniform. A uniform vaporization constant K' will also result in a uniform droplet radius τ as implied by Eq. (8). Therefore, if any three of these four variables have uniform distribution, the fourth one will also be uniform. It follows that all of these variables will remains uniform if they are initially uniform.

The independence of these variables from the radius r greatly simplifies the problem. k_f now has the normal meaning of the vortex strength. The partial derivative in Eq. (17) is thus essentially as same as the substantial derivative. Therefore h_1 can be determined from Eqs. (15 - 17) and is given by

$$h_1 = \frac{2\tau^2}{(1-K')(1+\beta')}(k_f^2+k_{fr})k_f \qquad (18)$$

where $\beta' = (1+\frac{3}{2}K')\beta$. The parameter g_1 can be obtained by the substitution of h into Eq. (15b), but it is considered less important and so is not considered further in this analysis.

The Lagrangian number density to zeroth order within the original cloud region can be determined from Eq. (7) by the substitution of U_r and is given by

$$n_f = \exp\left(-2\int_0^t \frac{(k_f^2+k_{fr})\tau}{(1-K')}\,dt\right) \qquad (19)$$

It is noted that this number density can be used in both the Lagrangian and Eulerian formulations since it is uniform within the cloud. Finally k_f, representing the momentum interaction between the gas and the cloud, is obtained by the substitution of Eqs. (18,19) into Eq. (17) and then integrating. It follows that

$$k_f = k_{f0}\frac{1+\beta'}{1+\beta_0'}\exp\left\{\int_0^t -\frac{n_f}{1+\beta'}\frac{d}{dt}\left[(1+\frac{3}{2}K')\frac{\beta_0\tau^{3/2}}{\rho_g}\right]dt\right\} \qquad (20)$$

where k_{f0} is the initial vortex strength. In general $k_{f0}=1$ for droplets whose initial speed equals the gas velocity. For initially stationary droplets, k_{f0} represents the vortex strength which exists after the droplets have been accelerated to the gas velocity, and may be approximated by $1/(1+\beta_0)$ based on the invariance of total angular momentum.

The exponential term in Eq. (20) represents the effect of droplet vaporization on the vortex strength, which is unity for the non-vaporizing case but is greater than one for the vaporizing case. For the non-vaporizing case (as in a saturated cloud), Eq. (20) may be further reduced to an algebraic equation after some mathematical manipulations so that

$$\left(1-\frac{\Delta}{\beta_0}\right)\exp\left(\frac{\Delta}{1+\beta_0}\right) = \exp\left(-\frac{2k_{f0}^2 t}{(1+\beta_0)^2}\right) \qquad (21)$$

where $\Delta = (k_{f0}-k_f)/k_f$

The vortex strength k_f in Eqs. (20) is not determined explicitly since n_f is also a function of k_f. However, Eq. (21) can be used to determine the variation of k_f with time easily. Furthermore, as $t \to \infty$, $\beta' \to 0$ and k_f can then be obtained from Eq. (20) for the non-vaporizing case.

$$k_{f\,t\to\infty} = \frac{k_{f0}}{1+\beta_0} \qquad (22)$$

The extent of the influence of droplets on the gas flow is now evident. For the initial loading ratio $\beta_0 < 0.1$, the decrease of the vortex strength (and hence the gas velocity) is less than 10%.

2. Potential Vortex Cloud

Following the procedures in the analysis of the forced vortex, the gas and droplet velocities in the potential vortex can be expressed as

$$V_\theta = k_p/r, \qquad V_{pr} = \tau k_{pr}/r^3 \qquad (23a,b)$$

$$U_\theta = q(t)/r, \qquad U_r = \tau p(t)/r^3 \qquad (24a,b)$$

where k_p, k_{pr}, p, q are considered as general functions of (r,t). k_{pr} is small compared with k_p and equal to zero for the non-vaporizing case. After substitution, Eqs. (5) and (9) become

$$\frac{dq}{dt} = \frac{1}{\varepsilon_v\tau}(k_p - q) \qquad (25a)$$

$$\frac{dp}{dt} = \frac{1}{\varepsilon_v\tau}(q^2 - (1-K')p + k_{pr}) + \frac{3\tau p^2}{r^4} \qquad (25b)$$

$$\frac{\partial k_p}{\partial t} = -\left(1+\frac{3}{2}K'\right)\frac{\beta}{\varepsilon_v\tau}(k_p - q) \qquad (26)$$

To zeroth order in ε_v solutions are $q \approx k_p$, $p \approx (k_p^2 + k_{pr})/(1-K')$. To first order in ε_v the solution is $q = k_p - \varepsilon_v q_1$ where

$$q_1 = \frac{k_{pr}\tau^2}{1+\beta'} \frac{1}{r^3} \frac{\partial k_p}{\partial r} \tag{27}$$

Therefore, the gas-droplet interaction in the potential vortex is mainly associated with the small radial velocity (Stefan flow) of the gas. This situation is unlike the forced vortex where the droplet velocity lag is mainly determined by the vortex strength rather than by the Stefan flow. Moreover, the number density in the potential vortex of the non-vaporizing cloud has been shown[14] to be typified by a high density front at the location of $r = (4t)^{1/4}$ moving outward from the center of the vortex. Even though k_{pr} is yet unknown, it is small so that the details of the interaction between the vaporizing cloud and the radial velocity within the potential vortex, though more complex, have only a small influence on the flow.

However, for the non-vaporizing case, $k_{pr} = 0$ so that $q_1 = 0$, the droplets will move with the same tangential speed as the gas. The drag force due to droplets on the gas flow is therefore zero and the variation of the velocity with time will be completely due to viscous dissipation. The solution of Eq. (9) at any finite time with the boundary condition of $rV_\theta = 0$ at $r = 0$ is then given by

$$V_\theta = \frac{k_{p0}}{r}\left[1 - \exp\left(-\frac{r^2}{4\sigma t}\right)\right] \tag{28}$$

$$\text{or} \quad k_p = k_{p0}\left[1 - \exp\left(-\frac{r^2}{4\sigma t}\right)\right] \tag{29}$$

Here k_p is not uniform so that it does not represent the ordinary vortex strength. Also, $k_{p0} = 1$ for droplets with the initial speed of the gas velocity, and $k_{p0} \approx 1/(1+\beta_0)$ for initially stationary droplets. In the case of $\sigma << 1$, the characteristic time for the motion of the high droplet density front is much smaller than the characteristic viscous vortex decay time. This implies that the droplet cloud constantly moves in a "clean" vortex field. The number density distribution is thus as same as the one calculated using $k_p = 1$ instead of Eq. (29). For the non-vaporizing cloud in Eulerian coordinates, the dimensionless number density is then given by[14]

$$n_p = \frac{r}{(r^4 - 4t)^{1/4}} \tag{30}$$

This result implies that the number density within the potential vortex becomes highly nonuniform.

NUMERICAL SOLUTIONS

Numerical solutions were carried out for the non-vaporizing case. The Stokes drag assumption was not made in numerical computation so that the Reynolds No. needs to be expressed in terms of dimensionless variables, and is given by

$$\mathrm{Re} = \left(18\frac{\bar{\rho}_{g0}}{\bar{\rho}_d}\frac{\tau}{\sigma}\right)^{1/2} \rho_g \left[\varepsilon_v (V_r - U_r)^2 + (U_0 - V_\theta)^2\right]^{1/2} \tag{31}$$

The values of density ratio $\bar{\rho}_d/\bar{\rho}_{g0} = 1000$, $\varepsilon_c = 10^{-4}$, $\varepsilon_v = 0.001, 0.01, 0.1$ and loading ratios $\beta_0 = 0.1, 1.0, 5.0$ were used in calculations. The Lagrangian Eqs. (5,6) for the droplet motion were integrated using fourth order Runge-Kutta method. The initially uniformly distributed droplets are separated by a distance $\bar{l}_0$ which is related to $\bar{n}_0$ by $\bar{n}_0 = 1/\bar{l}_0^3$. The gas field is discretized along the radial direction into several annular cells. The gas momentum Eq. (9) in each cell j is differenced in an explicit form given by

$$\frac{1}{\Delta t}(V_{\theta j}^{n+1} - V_{\theta j}^{n}) = -\frac{\beta_0}{\varepsilon_v}\frac{1}{n_0 \upsilon_j}\sum_{i=1}^{N_j}(V_{\theta j}^{n} - U_{\theta i}^{n}) f(\mathrm{Re}_i^n) + (\mathrm{Diffusion})_j^n \tag{32}$$

Here the diffusion term is center-differenced, υ_j is the volume of the discrete cell j, and N_j is the number of droplets in the cell j. The subscript i represents each droplet. The superscript n represents the time step. The collective droplet drag in each annular cell is assumed to act uniformly on that cell.

The computational cycle for each time step starts by determining a new value of the gas velocity from Eq. (32), and then solving Eqs. (5,6) using the new value of the gas velocity. The computational domain covers the region of $r \le 20$ which is considered large enough for obtaining good solutions in $r \le 1$. The convergence criterion generally requires $\Delta t < \min[3\varepsilon_v(\Delta r)^2/(4\beta_0\varepsilon_c), 2\varepsilon_c]$. For the fixed value of ε_c, the discrete cell width $\Delta r = 0.01$ and time $\Delta t = 0.1\varepsilon_v$ are used through all for simplicity despite of the additional computer time. The smaller time step is even required for the droplets close to the center of the potential vortex in the initial few time steps. The computation was performed until all droplets move out of the initially distributed region or until $t = 10$.

Figure 2 shows the variation of the computed vortex strength k_f with the radius during the time $t = 0 \sim 5$. The corresponding $\sigma = 0.667\times10^{-2} << 1$ explains two facts in the figure : (1) the k_f, even decreases, but remains about uniform in the region $r \le 1$, (2) the cloud expansion speed is much faster than the viscous diffusion speed, which can be seen from the figure that the cloud boundary expands up to $r = 1.55$ at $t = 0.5$ and the region outside the cloud still remains undisturbed, i.e., $k_f = 1$. The decreasing rate of k_f is also shown to decrease with time.

The variation of the computed k_f at $r = 0.8$ with time is compared with analytical solutions in Figs. 3 and 4. It is shown that for $\beta_0 = 0.1$ all droplets move out of the cloud before $t = 10$. The influence of the viscous diffusion on the cloud is more serious for the initially stationary cloud than the cloud with the initial speed of gas velocity. For $\varepsilon_v = 0.01$, even if $\beta_0 = 5$ (the corresponding $\sigma = 0.0333$), Fig. 3. shows that analytical solutions almost coincide with exact numerical solutions. Moreover, even though the assumption of $\varepsilon_v << 1$ has been made in the droplet dynamics equations, both figures show that the analytical solutions for $\varepsilon_v = 0.1$ are also acceptable and even more accurate than for $\varepsilon_v = 0.01$ in the cloud of $\beta_0 = 5$. For the case of $\varepsilon_v = 0.001$ the numerical solutions display the importance of the viscous diffusion from the ambience if $\sigma \geq O(1)$. In Fig. 4 the results for stationary droplet clouds show that momentum exchange mainly occurs in the initial short time during which droplets are accelerated to the gas speed.

The gas velocity distribution in the potential vortex is shown in Fig. 5 for the case of $\varepsilon_v = 0.01$ and $\beta_0 = 1$. The difference between the analytical solutions of Eq. (29) and the numerical solutions is almost not distinguishable. The vortex decay is therefore determined by the gaseous viscous stress. For other cases, as long as $\sigma << 1$, similar results will be obtained.

Summary and Conclusions

A dimensionless parameter ε_v, equal to the square of Stokes number, was found in a previous study to characterize the single droplet motion in axisymmetric forced and potential vortex flows. In the present study the characteristic cloud expansion time scale $\bar{\tau}_0/\varepsilon_v$ was identified so that another dimensionless parameter σ, equal to the ratio of the cloud expansion time to the viscous diffusion time, was found to characterize the behavior of a two-phase droplet cloud in swirling flows. The cloud behavior is then categorized into three different regimes according to the magnitude of σ. The momentum interaction, generally ignored in the regime $\sigma >> 1$ and the stationary cloud, is essential in the regime $\sigma << 1$ in determining the cloud motion as well as the vaporization and combustion. Analytical solutions of the gas velocities developed for the regime $\sigma << 1$ were found in excellent agreement with exact numerical solutions.

In the forced vortex, analytical solutions for $\sigma << 1$, so the diffusion effect is neglected, indicate that four variables (K, k_f, n, τ) continue to remain uniform in the initial cloud region if they are initially uniform. An algebraic equation of k_f for the non-vaporizing case was developed so that the variation of k_f with time could be easily obtained for various β_0's. As $t \to \infty$, the vortex strength decreases by a factor $1/(1+\beta_0)$. This implies that the gas-droplet interaction may be neglected for droplet clouds as dilute as $\beta_0 \leq 0.1$. Exact numerical calculations showed these analytic relations to be reasonably accurate for $\sigma << 1$ even if $\varepsilon_v = 0.1$.

In the potential vortex, the gas-droplet interaction is mainly associated with Stefan flow. Therefore, for the non-vaporizing case, the droplets essentially move in a non-interactive mode if droplet collisions are not considered. The decay of the potential vortex is thus only caused by the viscous dissipation in itself. For the regime $\sigma << 1$, the droplet cloud moves much faster than the viscous dissipation speed so that the droplet number density can be determined by the "clean" vortex flow.

Even though the parameter σ in this study is only used to characterize the motion of a droplet cloud, it certainly has implications for the cloud vaporization behavior considering $Pr = O(1)$. For the loading ratio $\beta_0 = O(1)$, σ can be expressed as the ratio of ε_c to ε_v. The parameter ε_c, i.e., the inverse of the group combustion number, has already played an important role in the cloud life time of a vaporizing or burning droplet cloud. It is therefore anticipated that the relative magnitudes of ε_c and ε_v will determine the vaporization behavior of a swirling droplet cloud.

The swirling flows occurring in spray vaporization or combustion will generally be far more complex than the simple vortices considered here. However, the results for $\sigma << 1$ suggest that a "strong" swirling flow will substantially influence the structure of the group vaporization or combustion

REFERENCES

1. McCreath,C.G., and Chigier,N.A., "Liquid Burning in the Wake of a Stabilizer Disk" *Fourteenth Symposium (International) on Combustion*, 1973, pp.1355-1363.
2. Onuma,Y., and Ogasawara,M., "Studies on the Structure of a Spray Combustion Flame", *Fifteenth Symposium (International) on Combustion*, 1974, pp.453-465.
3. Suzuki,T., and Chiu,H.H., "Multi-droplet Combustion of Liquid Propellants", *Proceedings. of Ninth (International) Symposium on Space Technology and Science*., Tokyo, Japan, 1971, pp.145-154.
4. Chiu,H.H., and Liu,T.M., "Group Combustion of Liquid Droplets", Combustion Science and Technology, Vol.17, 1977, pp.127-142.
5. Correa,S.M., and Sichel,M., "The Boundary Layer Structure of a Vaporizing Fuel Cloud", Combustion Science and Technology, Vol.28, 1982, pp.121-130
6. Correa,S M., and Sichel,M., "The Group Combustion of a Spherical Cloud of Monodisperse Fuel Droplets", *Nineteenth Symposium (International) on Combustion*, 1982, pp.981-991.

7. Annamalai,K., and Ramalingam,S.C., "Group Combustion of Char/ Carbon Particles", Combustion and Flame, Vol.70, 1987, pp.307-332.
8. Bellan,J., and Harstad,K., "Analysis of the Convective Evaporation of Nondilute Clusters of Drops", Int. J. Heat Mass Transfer, Vol.30, No.1, 1987, pp.125-136.
9. Bellan,J., and Harstad,K., "The details of the Convective Evaporation of Dense and Dilute Clusters of Drops", Int. J. Heat Mass Transfer, Vol.30, No.6, 1987, pp.1083-1093.
10. Attya,A.M., and Whitelaw,J.H., "Measurements and calculations of preheated and unpreheated confined kerosene spray flames", Combustion Science and Technology, Vol.40, 1984, pp.193-215.
11. Mao,C.P., *Wang,G.*, and Chigier,N.A., "An Experimental Study of Air-Assist Atomizer Spray Flame", *Twenty-first Symposium (International) on Combustion*, 1986, pp.665-673.
12. *Karagozian,A.R., and Marble,F.E.*, "Study of a Diffusion Flame in a Stretched Vortex", Combustion Science and Technology, Vol 45, 1986, pp.65-84.
13. Baum,H.R., Corley,D.M., and Rehm,R.G., "Time-Dependent Simulation of Small Scale Turbulent Mixing and Reaction", *Twenty-first Symposium (International) on Combustion*, 1986, pp.1263-1270.
14. Yang,M.H., and Sichel,M., "The Behavior of a Dilute Cylindrical Droplet Cloud in Swirling Flows", to be published elsewhere.
15. Kriebel,A R., "Particle Trajectories in a Centrifuge", J. of Basic Eng., Trans. ASME, Vol.83, 1961, pp.333-340.
16. *Hirschkron,R., and Ehrich,F F.*, "Entrained-Particle Trajectories in a Swirling Flow", ASME Winter Annual Meeting, Paper No.64-WA/FE-30, Nov. 1964.
17. Snow,J.T., "On the Formation of Dust Sheaths in Tornado Vortices", *13th Conference on Severe Local Storms*, American Meteorological Society, 1983, pp.70-73,
18. Bellan,J., and Cuffel,R., "A Theory of Nondilute Spray Evaporation based upon Multiple Drop Interactions", Combustion and Flame, Vol.51, 1983, pp.55-67.
19. Yang,M.H., and Sichel,M., "Particle Motion in Vortex Flow", Twentieth Fall Technical Meeting, Eastern Section of the Combustion Institute, 1987.
20. Crowe,C.T., "Review - Numerical Methods for Dilute Gas-Particle Flows", J. of Fluid Engineering, Trans. ASME, Vol.104, 1982, pp.297-303.
21. Soo,S.L., *Fluid Dynamics of Multiphase Systems*, Blasidell Publishing Co., Waltham, MA, 1967, p.33.
22. Rudinger,R., *Fundamentals of Gas-Particle Flow*, Handbook of Power Technology, Vol.2, Elsevier Scientific Publish-ing Co., 1980, pp.7-11.

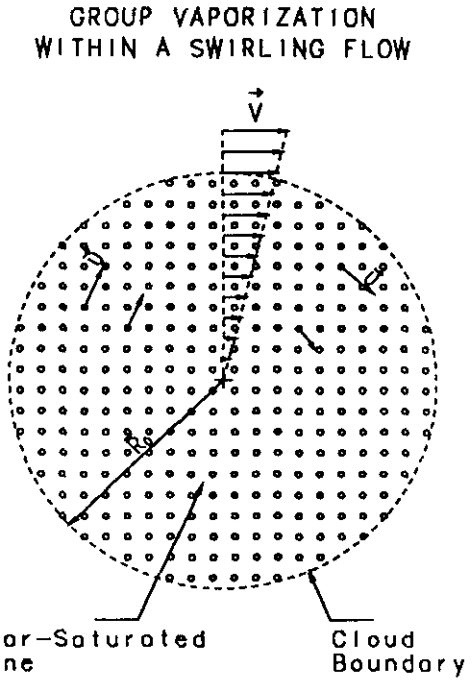

Fig.1 Physical picture of a cylindrical droplet cloud in a swirling flow of an infinite region.

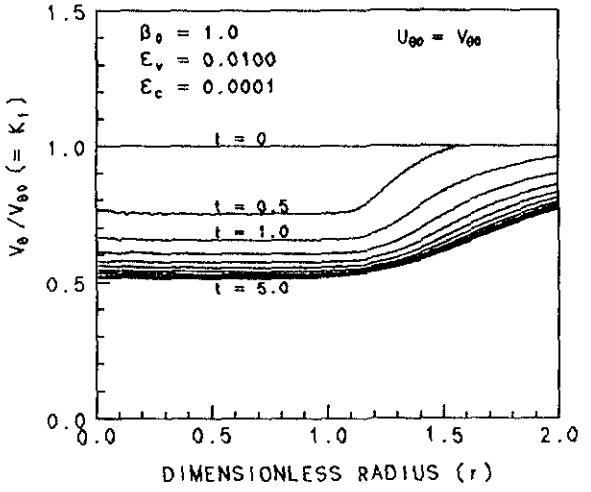

Fig.2 Profiles of the computed dimensionless forced vortex strength during t = 0 ~ 5.

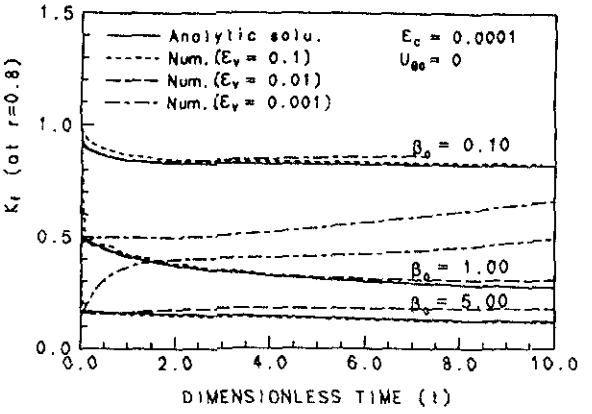

Fig.4 Comparison of analytical solutions with numerical solutions of the dimensionless forced vortex strength at r = 0.8 for $U_{\theta 0}$ = 0.

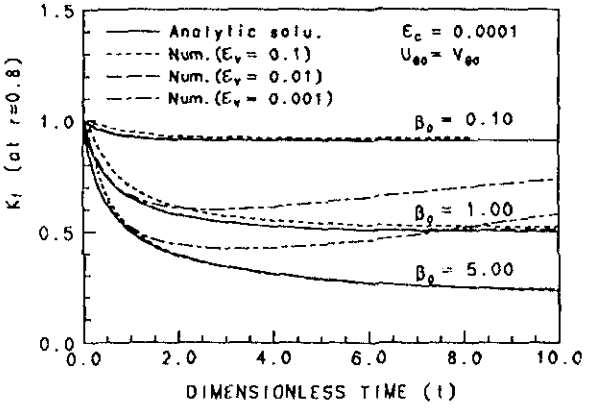

Fig.3 Comparison of analytical solutions with numerical solutions of the dimensionless forced vortex strength at r = 0.8 for $U_{\theta 0} = V_{\theta 0}$.

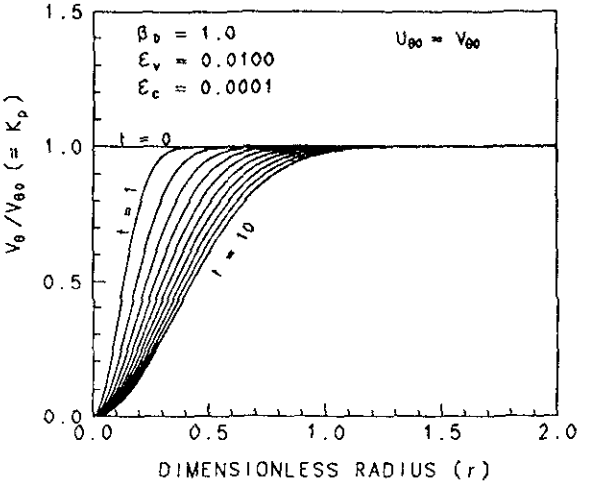

Fig.5 Comparison between analytical and computed profiles of k_p during t = 0 ~ 10.